ACADEMIA ROMÂNĂ
Revue Roumaine de Chimie
https://www.icf.ro/rrch/

Rev. Roum. Chim.,
2024, *69*(10–12), 585–593
DOI: 10.33224/rrch.2024.69.10-12.08

ADSORPTION OF METHYLENE BLUE BY (Co, Cu, Zn AND Ce)-MODIFIED ZSM-5 MOLECULAR SIEVE

Jie YANG,[a,b,*] Jinlei MENG,[a,b] Jingjing SHI,[a] Xuechun SONG[a,b] and Tao CHEN [a]

[a]School of Energy Materials and Chemical Engineering, Hefei University, Hefei, Anhui, 230601, China
[b]Carbon Neutrality and Carbon Peaking Materials and Resource Chemical Laboratory, Hefei University, Hefei, Anhui, 230601, China

Received February 28, 2024

A novel ZSM-5 zeolite modified by Co, Cu, Zn, and Ce was synthesized by impregnation method to remove the industrial toxic dye methylene blue from water using a sunlight-assisted adsorption process. When the pH value is 8, the dosage of adsorbent is 5.0mg, and the adsorption is three hours, the adsorption effect of the adsorbent reaches 82%, the adsorption capacity reaches the equilibrium in 10 minutes, and the maximal theoretical adsorption amount of the mixed modified adsorbent is 124.0mg·g^{-1}. This study shows that the modified ZSM-5 molecular sieve is an efficient adsorbent.

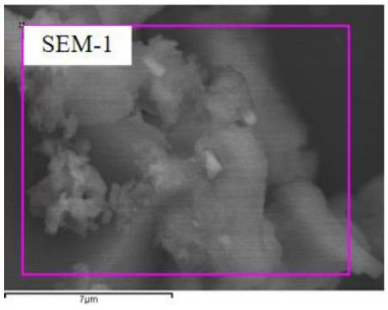

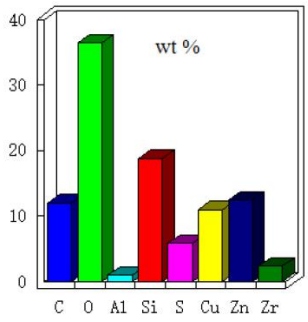

INTRODUCTION

Dyes are an indispensable part of modern life and are involved in many industries, including textiles, paper, and food, with leather, cosmetics, and printing being the main industries. The colored wastewater from industries is the main pollutant in the production process and commonly contains large quantities of pollutants that flow into lakes and rivers without prior treatment. Such pollutants, if not treated at the primary level, will cause unimaginable harm to the environment. And it poses a significant threat to humans, animals, and water bodies.[1,2] Even discharging colored wastewater in insufficient concentrations into the water can seriously affect the ecology of the waters. Methylene blue is widely used in chemical dyes, natural dyes, and dyestuffs. It is relatively stable in air, but its aqueous solution is alkaline and toxic. Because it is widely used and unfriendly to the environment, treating wastewater containing methylene blue has increasingly attracted people's attention.[3,4]

Adsorption membrane separation, electrochemical oxidation, and chemical precipitation are the most commonly used techniques for the removal of dyes such as methylene blue from industrial wastewater. Among

* Corresponding authors: yangjhfuu@163.com

them, the adsorption method has the advantages of simple operation, low cost, wide adaptability, and high recovery rate. In the study of methylene blue wastewater adsorption, a kind of efficient and practical adsorbent was found to be a research field worth exploring.[5,6]

Zeolites are effective adsorbents that can be easily synthesized from a variety of precursor materials in an environmentally friendly and economical way.[7,8] Especially ZSM-5 molecular sieve has good chemical inertness and biocompatibility, ZSM-5 has a porous structure and large specific surface area, it can effectively adsorb nitrogenous dyes in water, and is often used as an adsorbent for wastewater.[6,9] In this study, ZSM-5 molecular sieves were synthesized by a metal doping modification to obtain higher adsorption properties.

The introduction of metal ions allows a better synergy between Lewis bases and Lewis's acids on the catalysts. In general, the introduction of metal ions does not change the crystal structure of molecular sieves, and the activity of the metal skeleton form is higher than that of the non-skeleton form, so the doping of metal ions into the molecular sieve skeleton is an area worth exploring.[10,11]

In this study, the metal ion activity of (Zn, Co, Cu, Ce) and the surface adsorption of ZSM-5 were used to dope the metal ions into the framework of molecular sieves by leaching method, to characterize its structure and to study its adsorption performance on methylene blue (MB) in the hope of providing a reference for the selection of adsorbents for organic dyes wastewater treatment.

EXPERIMENTAL

ZSM-5 Synthesis

Huang *et al*. (2000) and Frunz *et al*. (2006) found that extended gel aging at 25℃ increased the amount of ZSM-5 precursors.[12,13] Selvin *et al*. (2011) and Goncalves et al. (2008) aged ZSM-5 gels at various temperatures and periods.[14,15] ZSM-5 catalyst prepared by hydrothermal synthesis method.[16–20] Add 1.2 g NaOH, 3.5g tetra-n-butyl ammonium bromide, and 1.1g $Al_2(SO_4)_3 \cdot 18H_2O$ to a 150 mL beaker and dissolve in 100 mL deionized water. Then add 24.0 g SiO_2, stir for 20 min, and transfer the solution to a stainless steel hydrothermal reactor, a constant temperature of 180 ℃ in an oven to dry for 72 h. Cool, wash, and filter until the filtrate becomes neutral and is transferred to the crucible. The filtrate is dried overnight at a constant temperature of 120 ℃. Then it is taken out and calcined at 650 ℃ in the high-temperature furnace.

Preparation process of metal ion doped molecular sieve

A certain amount of cerium sulfate, cobalt chloride, zinc sulfate, and copper sulfate were dissolved in 500 mL anhydrous ethanol by the equimolar impregnation method, then 2.0 g ZSM-5 molecular sieve was added, followed by a 30 min ultrasonic wave and two hours stirring to make the molar ratio of the modified dopant 2.5 wt%.[21,22] Dilute hydrochloric acid was added (1.0 mL concentrated hydrochloric acid was added into 9.0 mL deionized water and diluted to 10.0 mL) to adjust the pH value to about 5. It was stirred and impregnated at room temperature for 24 h, dried in a drying oven at 120 ℃ for six hours, washed three times in deionized water, and filtered. Then the samples were put into the crucible and calcined at 550 ℃ in the horse boiler for five hours, then cooled and preserved.

Characterization of ZSM-5 and its metal modification

The crystal structure was determined by X-ray diffractometer (XRD, Rigaku Model, Japan, TD-3500) using a Cu-Kα target (wavelength 1.542 nm) in the range of 5°~70° (2θ). The morphology and structure were observed by emission scanning electron microscope (SEM, Zeiss Sigma 300). The functional group structure was tested by Fourier transform infrared spectrometer (FT-IR-8400S Shimadzu) when the wave number was 600 cm^{-1}~4000 cm^{-1}, using KBr slices, and the surface characteristics were analyzed by nitrogen adsorption-desorption isotherm of BET specific surface area. The relationship between the quantity, physical properties, and temperature change was measured by TG-DTA (Q500, TA Instruments).

RESULTS AND DISCUSSION

Analysis of Morphology

Figure 1 shows the SEM photographs of the zeolites doped with different metal ions respectively after roasting, characterizing the apparent morphology of the metal ion-doped ZSM-5 zeolites. From the figure, it can be seen that the ZSM-5 molecular sieves have cubic crystal structures with good shape, smooth particle surfaces, and precise angles. The surface of the molecular sieves containing metal ions is rough and the morphology changes. The particle morphology shows a multidirectional growth trend. The volume increases and the particles become wider. Round et al. attributed this phenomenon to the homogeneous substitution of

metal ions on ZSM-5 molecular sieves, where metal ions such as Ce, Co, Zn, Cu, etc., enter into the framework of the molecular sieves to change their morphology.[23]

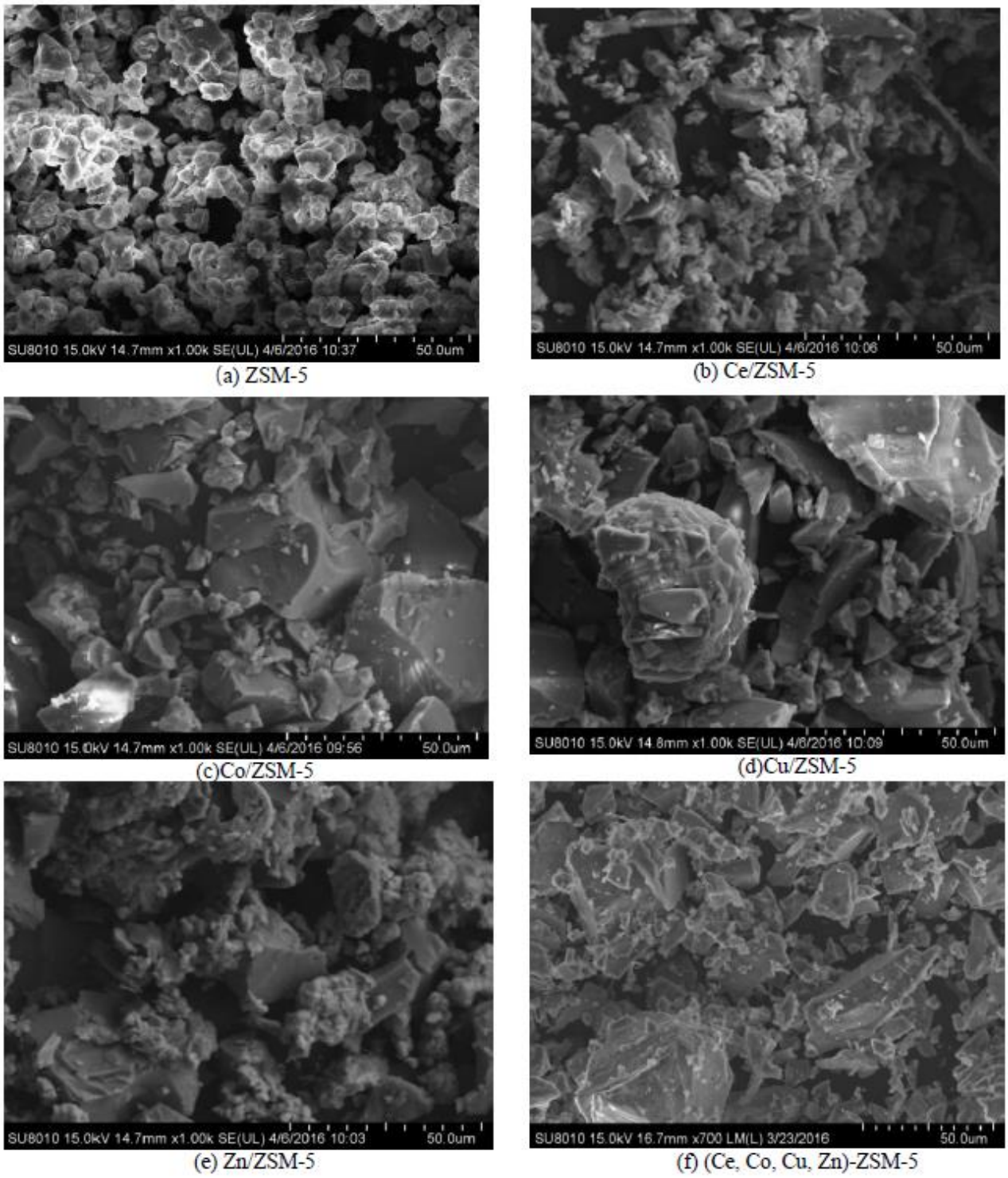

Fig. 1 – SEM images of: a) – ZSM-5; b) – Ce/ZSM-5; c) – Co/ZSM-5; d) – Cu/ZSM-5; e) – Zn/ZSM-5; f) – (Ce, Co, Zn, Cu)-ZSM-5, after roasting.

From the EDS spectra, it can be seen that the catalysts in Figs. 2 and 3, in addition to the basic elements silicon, oxygen, aluminum, and other elements, have cerium and zinc covering the surface, indicating that the metal ions Zn (16%) and Ce (48%) have entered the molecular sieve and correspond to

the diffraction peaks of XRD. From SEM and EDS, it can be observed that some metal ions have entered the framework of the molecular sieve, while others have covered the surface of the molecular sieve, altering its appearance. However, impurities such as S, Zr, and Cu appeared in the quantitative analysis results. Due to the proximity of many samples during testing, contamination occurred.

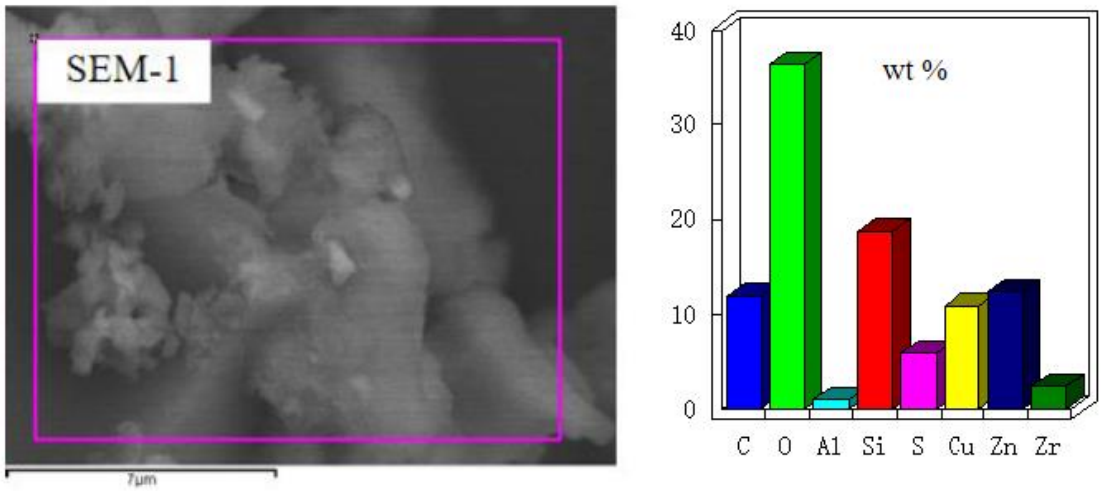

Fig. 2 – EDS photos and energy spectrum analysis of Zn-ZSM-5 catalyst (quantitative analysis results).

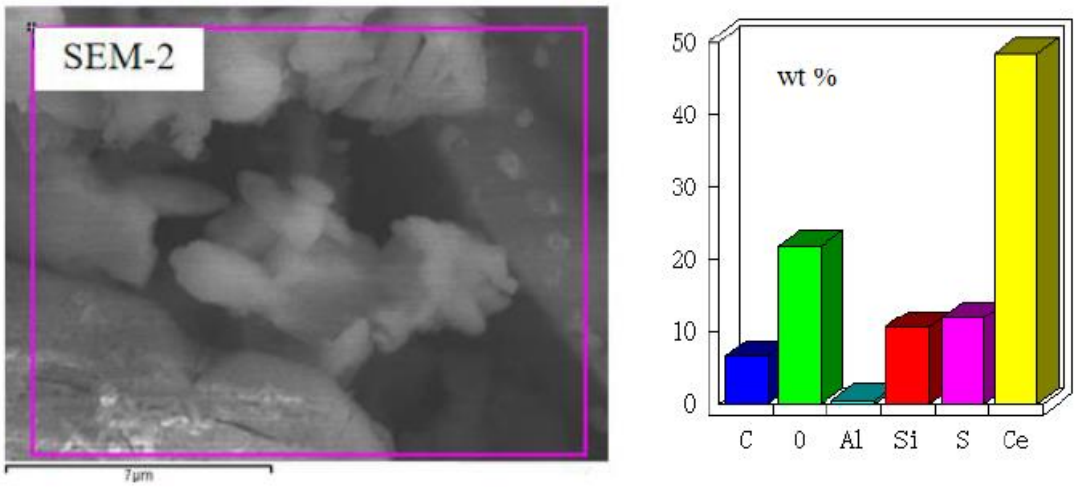

Fig. 3 – EDS photos and energy spectrum analysis of Ce-ZSM-5 catalyst (quantitative analysis results).

XRD Analysis

The angles of ZSM-5 and ZSM-5 doped metal ions are indicated by (5°~70°) XRD spectra. In **Fig.4**, the essential characteristic peaks of ZSM-5 were retained, indicating that the addition of metal ions did not cause too much damage to the structure of the molecular sieves, and the overall crystallinity was high. From the overall diffraction angles of 2(a), 2(e), and 2(f), the peaks in the plots are sharper, with higher dispersion of metal ions Zn and mixed doped metal ions. Compared with (a) ZSM-5, (d) Cu-ZSM-5 exhibits distinct CuO characteristic peaks (35.5, 38.6), suggesting that copper oxide particles were formed during the preparation of Cu-ZSM-5 molecular sieves. Compared to 2(c) and 2(a), the absence of peaks indicates that Co enters the ZSM-5 molecular sieves, and the interactions between the peaks cancel out their individual effects and greatly reduce the crystallinity. This is since the radius of Co ions is larger than that of Si ions, which partially replaces the Si ions, leading to a decrease in crystallinity.[24]

Figure 4b shows a weaker peak compared to Fig. 4a, with no aggregated diffraction peaks of metals or metal oxides, which is due to the incorporation of metal ions resulting in higher X-ray diffraction absorption coefficients of the molecular sieves.[25] In addition, the presence of

stray peaks in the XRD spectrum indicates that the sample is impure and contaminated.

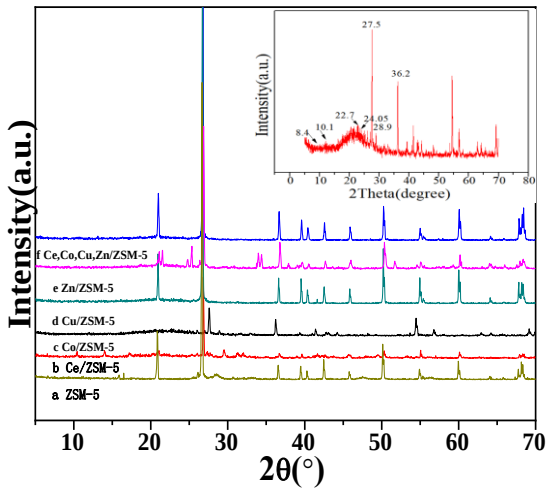

Fig. 4 – XRD spectrum of: a) ZSM-5; b) Ce/ZSM-5; c) Co/ZSM-5; d) Cu/ZSM-5; e) Zn/ZSM-5; f) (Ce, Co, Cu, Zn)-ZSM-5.

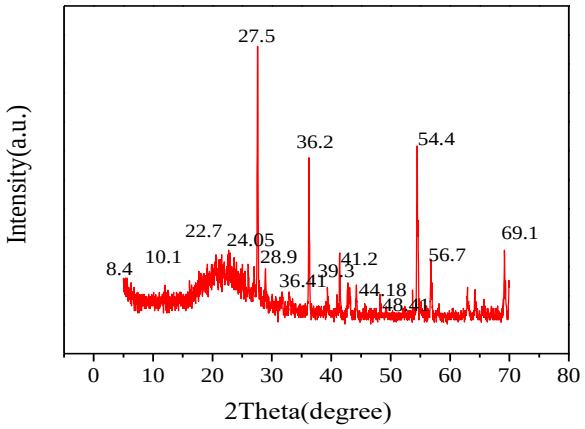

Fig. 5 – XRD spectrum of ZSM-5 catalyst.

The crystal structure was determined by X-ray diffractometer (XRD, Rigaku Model, Japan, TD-3500) using a Cu-Kα target (wavelength 1.542 nm) in the range of 5°~70° (2θ). All samples exhibited typical diffraction peaks associated with the ZSM-5 molecular sieve at 2θ = 8.0° (101), 8.9° (200), 23.2° (501), 24.0° (151) and 24.5° (303) (PDF#44-0003). ZSM-5 molecular sieve belongs to the orthogonal crystal series, with a = 2.017 nm, b = 1.996 nm, and c = 1.343 nm as the lattice parameters of the spatial group pnma. The comparison with the PDF library crystal plane values is consistent with the molecular formula of the crystal cell composition $Na_nAl_nSi_{96}–nO_{192}·16H_2O$. The results show that the material composition of the ZSM-5 molecular sieves is consistent with that of the ZSM-5 molecular sieves.

FTIR Analysis

Figure 6 shows the FT-IR spectra of loaded (Co, Ce, Zn, Cu) -ZSM-5 molecular sieves. It can be seen from the figure that the metal ion-doped ZSM-5 molecular sieves were synthesized by the impregnation method. The transmission peaks at 789 cm^{-1} and 1083 cm^{-1} are antisymmetric stretching vibration peaks of the Si-O-Si type. The transmission peak at 1230 cm^{-1} is the antisymmetric stretching vibration peak of the -SiO_4 tetrahedron in the ZSM-5 structure. The transmission peak at 1588 cm^{-1} corresponds to the characteristic vibrational peak of the Si-OH structure. the transmission peak between 3059~3500 cm^{-1} is a typical adsorption peak. As can be seen in Fig. 6, the Fourier transform infrared spectra of ZSM-5 molecular sieves doped with different metal ions are the same as those of ZSM-5,[26–29] indicating that the structure of the molecular sieves is not damaged by homocrystalline substitution.

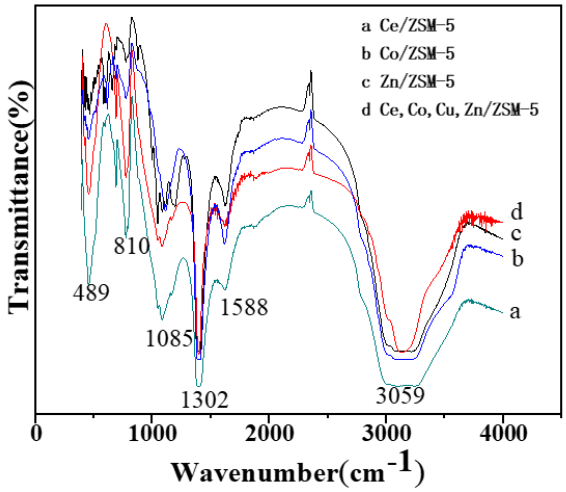

Fig. 6 – FT-IR spectrum of (Ce, Co, Cu, Zn)-ZSM-5.

TG-DTA Analysis

Figure 7 shows the TG-DTA curves of Co-ZSM-5 molecular sieves at 24 ℃~600 ℃. The weight loss process of Co-ZSM-5 molecular sieves is divided into three stages. In the second stage, decomposition and removal of the template is carried out at temperatures from 200 ℃ to 450 ℃. In the third stage, from 450 ℃ to 600 ℃, the remaining template can only be removed at high temperatures due to the strong interaction between the ammonium groups in the template and the organic matter.

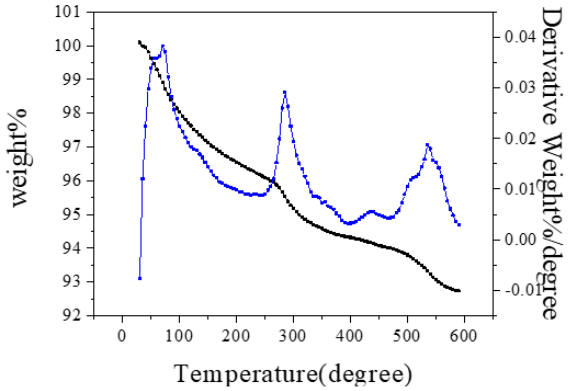

Fig. 7 – TG-DTA curve of Co-ZSM-5.

Figure 8 shows the TG-DTA curves of (Co, Cu, Ce, Zn)-ZSM-5 molecular sieves in the range of 24 ℃~600 ℃. The thermal weight loss process of (Co, Cu, Ce, Zn)-ZSM-5 molecular sieves is divided into three stages. In the second stage, the apparent weight loss peak occurs at 150 ℃~450 ℃, which is due to the formation of hydrogen bonds between the hydrogen atoms in copper sulfate and the oxygen atoms in the sulfate ions, and higher energy is required to disrupt this structure and the decomposition of the templating agent to remove it. In the third stage, between 45 ℃~60 ℃, the ammonium group in the templating agent has a strong effect on the organic matter, so the remaining templating agent can only be removed at high temperatures.

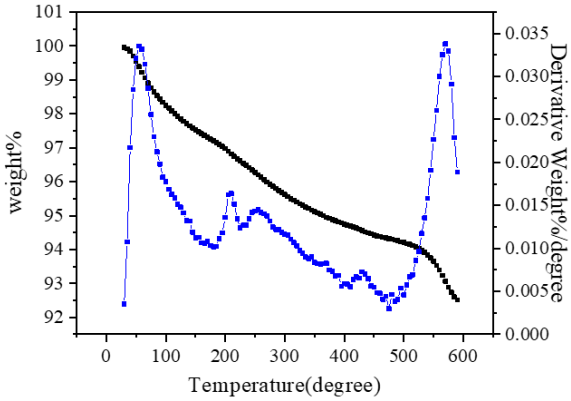

Fig. 8 – TG-DTA curve of (Co, Cu, Ce, Zn)-ZSM-5.

Nitrogen adsorption characterization

The specific surface area of the molecular sieve was calculated by BET to be 378 $m^2 \cdot g^{-1}$. It can be seen that the specific surface area of the (Co, Cu, Ce, Zn)-ZSM-5 molecular sieve decreased, but the pore size increased. The adsorption increases with the increase of relative pressure, which belongs to the N_2 adsorption-desorption curve.

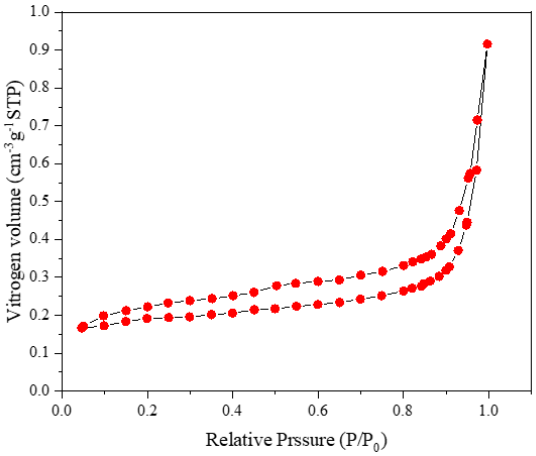

Fig. 9 – BET curve of (Co, Cu, Ce, Zn)-ZSM-5.

Following the modification, the changes in the properties of ZSM-5 are described in Table 1. Certainly, the reduction inthe specific surface area of the modified ZSM-5 molecular sieves is likely a consequence of the alteration or destruction of certain pore structures, which can be linked to the introduction of metal ions.[30]

Table 1

Different ZSM-5 molecular sieve pore parameters

Sample	Specific surface area [$m^2 \cdot g^{-1}$]	Total hole capacity [$cm^3 \cdot g^{-1}$]	Diameter of hole [nm]
ZSM-5	403	0.18	2.23
Co-ZSM-5	390	0.25	3.20
Cu-ZSM-5	392	0.23	3.78
Ce-ZSM-5	395	0.22	4.16
Zn-ZSM-5	396	0.22	3.82
(Co, Cu, Ce, Zn)-ZSM-5	378	0.16	2.05

Adsorption *Experiments*

A certain amount of modified ZSM-5 was added into 250 mL MB solution with a particular initial concentration, and the initial pH was adjusted. After a certain time of oscillating adsorption at constant temperature and speed, 50 mL of the adsorption solution was removed for separation by magnetic separation technology. The liquid was taken, and the concentration of MB was measured by ultraviolet/visible photometer (Shimadzu UV260). The adsorption capacity of ZSM-5 on MB was calculated by equation:

$$Q_T = \frac{(C_0 - C_T) \times V}{M}$$

Where, Q_T is the adsorption of MB by ZSM-5 at the adsorption time ($mg \cdot g^{-1}$); T is the adsorption

time (min); C_0 and C_T are the mass concentration of MB at the initial and adsorption time, respectively ($mg \cdot L^{-1}$); V is the volume of the MB solution (L); M is the quality of ZSM-5 (g).[21]

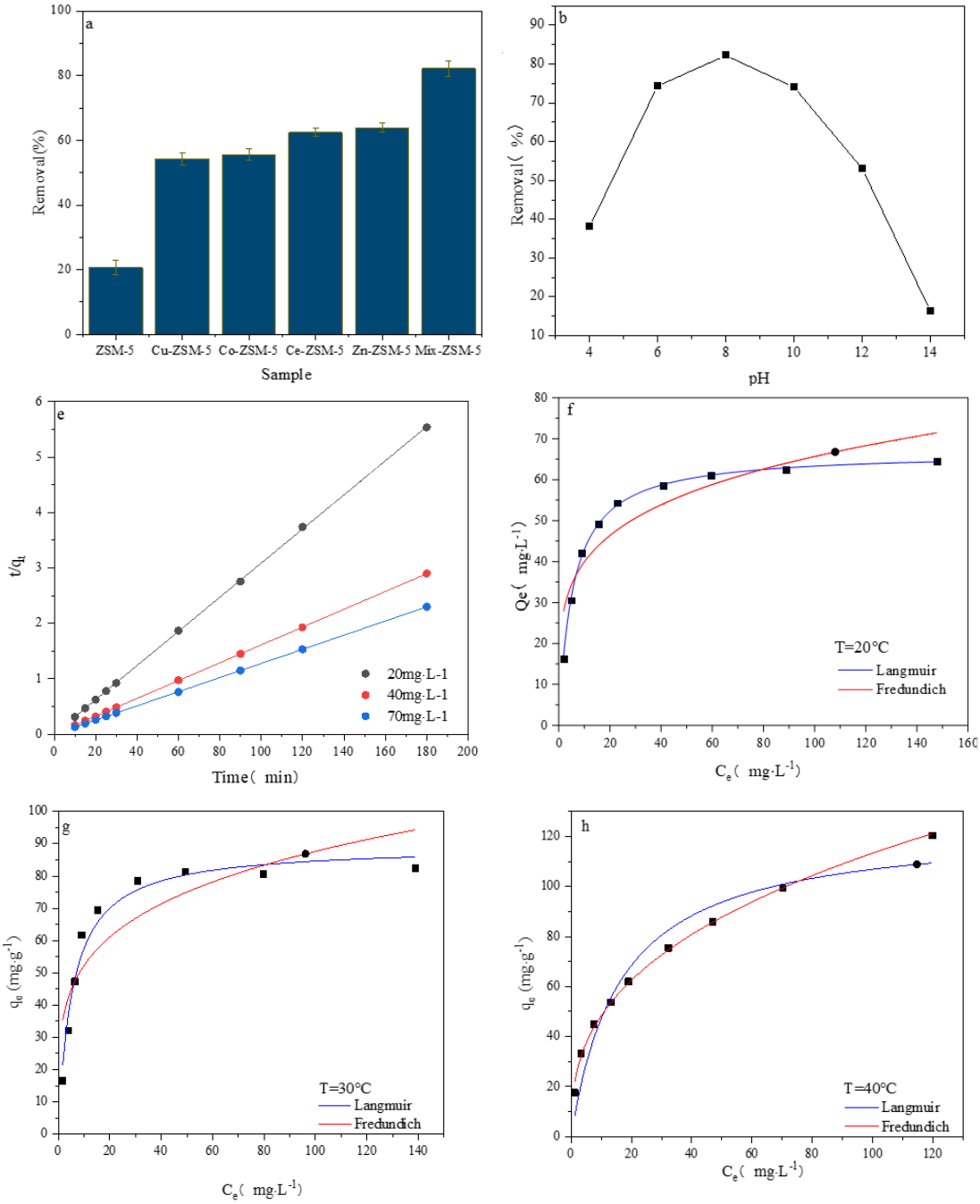

Fig. 10 – a) Impact of various ZSM-5 molecular sieve species on MB adsorption; b) Influence of varying pH levels on the efficacy of adsorption; c) Impact of the initial concentration of the MB solution on the efficiency of adsorption; d) and e) Kinetic modeling of Mix-ZSM-5; f), g) and h) Fitting of the Langmuir and Freundlich models.

Figure 10a shows the removal rates of six different groups of ZSM-5 molecular sieves under the same conditions, where the unmodified one has the lowest removal rate, and the mixed-modified one has the highest removal rate of 82%, showing better adsorption performance than the other molecular sieves.

pH is not only an important factor that affects adsorption, but also one of the factors that determines the dissociation of functional groups.[31]

Figure 10b depicts the removal rate of MB by hybrid modified molecular sieves at different pH values, it can be seen that acidic conditions have a greater impact on the removal rate of molecular

sieves, this is because MB is a cationic dye, there is a competition between H^+ and dye molecules adsorption, which affects the adsorption performance, the best adsorption performance is achieved when pH reaches 8, and continue to regulate pH, the trend of adsorption performance decreases more and more, this is because the OH^- corrodes molecular sieve pore structure and reduces its adsorption performance.

Figure 10c shows the study of the effect of different concentration gradients of mixed modified molecular sieves on the adsorption, it can be seen that the adsorption reached the adsorption equilibrium in about ten minutes, and the adsorption rate was fast.

The kinetics of MB adsorption by hybrid-modified molecular sieves is explored in Figs. 10d and e. The kinetic analysis shows that the saturated adsorption is positively correlated with MB concentration and is more in line with the second-order kinetic model.[32]

The adsorption isotherms of MB by the hybrid-modified molecular sieves are shown in Figs. 10g and h. The data were fitted with Langmuir and Fredundich models with the parameters shown in Table. As can be seen from the figures, the adsorption tends to increase with increasing temperature and concentration, indicating that the adsorption is a heat-absorbing process. Both models fitted the experimental data better, with Langmuir being more consistent with this adsorption process, and Fredundich's R^2 increased at increasing temperatures, which may be due to the movement of the active sites of the molecular sieves. According to the Langmuir model, the maximum theoretical adsorption was 124 $mg \cdot g^{-1}$ at 40 ℃.

CONCLUSIONS

ZSM-5 molecular sieve was prepared by hydrothermal synthesis with intact morphology and smooth surface. The Co-ZSM-5, Cu-ZSM-5, Ce-ZSM-5, Zn-ZSM-5, (Co, Cu, Ce, Zn)-ZSM-5 molecular sieves were synthesized by the impregnation method. The results show that doped metal ions do not change the framework of ZSM-5 zeolite. The morphology of the molecular sieves with metal ions was changed because the surface was rough. The appearance of the particles showed a multidirectional growth trend, and the volume increased, and the particles became wider. FT-IR and XRD results show that ZSM-5 zeolite doped with metal ions does not change the framework and structure of ZSM-5 zeolite, but doped with metal ions can improve the dispersion of ZSM-5 zeolite.

Through the simulation of the organic pollutants of metal-modified ZSM-5 molecular sieve by methylene blue and the experiment of the influence of ZSM-5 molecular sieve doped with metal ions on the catalytic degradation of methylene blue, it is concluded that the appropriate conditions for the adsorbent degradation of methylene blue doped with metal ions are as follows: pH = 8, the amount of adsorbent is 5mg. It was found that the adsorption capacity reached equilibrium in 10 min, and the (Co, Cu, Ce, Zn)-ZSM-5 adsorption capacity was 124$mg \cdot g^{-1}$.

Acknowledgements. This work was financially supported by the excellent young talents fund project in Universities of Anhui Province (gxyq2022072), Provincial Quality Engineering Demonstration Chemical Experiment Training Center Project (2022sysx024), Hefei University Undergraduate Quality Engineering Project (Chemical Experiment Teaching Team 2022hfujxtd04), 2023 Ministry of Education Industry University Research Collaborative Education Project (231006655105108).

REFERENCES

1. P. Kumar, R. Agnihotri, K. L. Wasewar, H. Uslu and C. K. Yoo, *Desalin. Water Treat.*, **2012**, *50*, 226–244.
2. M. A. Schoonen and J. M. T. Schoonen, *J. Colloid Interface Sci.*, **2014**, *422*, 1–8.
3. T. Tavangr, K. Jalali, M. A. A. Shahmirzadi and M. Karim, *Sep. Purif. Technol.*, **2019**, *216*,115–125.
4. L. Suhadolnik, A. Pohar, U. Novak, B. Likozar, A. Mihelic and M. Ceh, *J. Ind. Eng. Chem.*, **2019**, *72*, 178–188.
5. X. F.Liu, S. H. Zeng, R. W. Wang, Z. T. Zhang and S. L. Qiu. *Chem. Res. Chin. Univ.*, **2018**, *34*, 350–358.
6. J. Ding, S. Y. Fan, P. J. Chen, G. F. Zhao, Y. Liu and Y. Lu, *Catal. Sci. Technol.*, **2017**, *7*, 2087–2094.
7. D. Hu, Q. H. Xia, X. H. Lu, X. B. Luo and Z. M. Liu, *Mater. Res. Bull.*, **2008**, *43*, 3553–3561.
8. R. Khoshbin and R. Karimzadeh, *Adv. Powder Technol.*, **2017**, *28*, 1888–1897.
9. S. Wodarz, N. A. Slaby, M. C. Zimmermann, N. O. Thomas and S. Jrg, *Ind. Eng. Chem. Res.*, **2020**, *59*, 17689–17694.
10. J. W. Li, M. F. Ma, Q. W. Sun, W. Y. Ying and D. Y. Fang, *Fuel Process Technol.*, **2015**, *134*, 32–38.
11. Y. Fang, H. P. Zhang, X. P. Li, H. Huang, H. C. Xin, M. H. Lu, M. S. Li and X. B. Li, *Energy and Environment Focus*, **2014**, *3*, 227–235.
12. L. Huang, W. Guo, P. Deng, Z. Xue and Q. Li, *J. Phys. Chem. B*, **2000**, *104*, 2817–2823.
13. L. Frunz, R. Prins and G. D. Pirngruber, *Microporous Mesoporous Mater*., **2006**, *88*, 152–162.
14. M. L. Gonçalves, L. D. Dimitrov, M. H. Jordão, M. Wallau and E. A. Urquieta-González, *Catal. Today*, **2008**, *133–135*, 69–79.
15. R. Selvin, H.-L. Hsu, L. S. Roselin and M. Bououdina, *Synth. React. Inorg, Met.– Org, Nano-Met. Chem*., **2011**, *41*, 1028–1032.
16. D.-K. Nguyen, V.-P. Dinh and N. T. Dang, *RSC Adv*., **2023**, *13*, 20565-20574

17. Z. Chen, Z. Li, Y. Zhang, D. Chevella, G. Li, Y. Chen, X. Guo, J. Liu and J. Yu, *Chem. Eng. J*., **2020**, *388*, 124322.
18. A. Asghari, M. K. Khorrami and S. H. Kazemi, *Sci. Rep*., **2019**, *9*, 17526–17532.
19. P. Noor, M. Khanmohammadi, B. Roozbehani, F. Yaripour and A. Bagheri Garmarudi, *J. Energy Chem*., **2018**, *27*, 582–590.
20. A. A.-h. F. Lafi, S. K. Matam and H. A. Hodali, *Ind. Eng. Chem. Res*., **2015**, *54*, 3754–3760.
21. H. Wang, *Coatings*, **2022**, *12*, 1–11
22. M. L. Yu, H. Dong, Y. D. Zheng and W. P. Liu, *Chemosphere*, **2021**, *280*, 130567–130572.
23. C. I. Round, C. D. Williams and K. Latham, *Chem. Matter*., **2001**, *13*, 468–472.
24. S. L. Gao, Y. J. Wang and X. Diao, *Bioresource Technol.*, **2010**, *101*, 3830–3837.
25. N. Y. Kang, Y. K. Park and K. Chul, *B Korean Chem. Soc.*, **2018**, *39*, 1229–1249.
26. Y. Yang, Y. Yan, H. P. Zhang and X. W. Wu, *Sep. Purif. Technol*., **2020**, *237*, 116452–116460.
27. G. T. M. Kadja, M. D. Rukmana, M. D. Rukmana, R. R. Mukti, M. H. Mahyuddin, A. G. Saputro and T. D. K. Wungu, *Mater. Lett.*, **2021,** *290*, 129501–129508.
28. Y. P. Guo, T. Long, Z. F. Song and Z. A. Zhu, *J. Biomed. Mater. Res., Part B*, **2014**, *102*, 583–594.
29. A. R. K. Gollakota, V. S. Munagapati, V. Volli, S. Gautam, J. C. Wen and C. M. Shu, *J. Hazard. Mater.*, **2021**, *416*, 125925–125932.
30. Z. Zhang, Y. Chen, P. Wang, Z. Wang, C. Zuo, W. Q. Chen and T. Q. Ao, *J. Hazard. Mater*., **2021**, *423*, 127103–127110.
31. P. Monash and G. Pugazhenthi, *Korean J. Chem. Eng*., **2010**, *27*, 1184–1194.
32. M. Y. Chang and R. S. Juang, *J. Colloid Interface Sci***., 2004**, *278*, 18–24.